ISSN No: 2348-4845
International Journal & Magazine of Engineering, Technology, Management and Research
A Peer Reviewed Open Access International Journal

Design and Implementation of Two Axis Gimbal System

Majji Nagendra
Department of Electrical and Electronics Engineering,
BITS, Visakhapatnam,
Andhra Pradesh 530041, India.

Sai Ganesh Mopada
Department of Electrical and Electronics Engineering,
BITS, Visakhapatnam,
Andhra Pradesh 530041, India.

ABSTRACT:
For general image sensing applications in avionics, it is necessary to keep the line of sight (LOS) of the sensor insensitive to the carrier's body rates. Such application requirement necessitates the usage of an inertial stabilized plat-form (ISP). Any ISP generally consists of a two- or three-axis gimbal system with the payload, i.e., sensors or cameras on the inner gimbal. The dynamics of such a system are complicated, and it is a difficult task to attain the objective of stabi-lization. Parameter estimation techniques are used to derive a state space model of the gimbal system dynamics from the experimented data or design data of the gimbal system. In this paper, a state space model is estimated using a prediction error method for a cross-coupled two-axis inertial stabilization platform and the results of both cross-coupled and state space estimation method are compared. The model satisfies the characteristics of the original system for a required frequency range.

Keywords: ***Inertial stabilized platform; Gimbal systems; Parameter optimization; Line of sight retention.***

1. Introduction:

Every image sensing and target tracking application requires an image processing device which is supposed to follow and track the target with high precision. Such devices are generally placed on moving vehicles which cause disturbances in the line of sight (LOS) of sensor and also degrade the quality of the image. Inertial stabilized platforms (ISP) are employed for the purpose of decoupling the movement of the body from the sensor's LOS [1]. The sensor will be placed in the inner elevation gimbal, and they are carried by the outer azimuth gimbal. The dynamics of such a structure are derived using Newton's second law or Lagrange equations [2, 3]. These equations are hard to derive if one assumes a dynamic mass imbalance in the system.

Several papers have been published on gimbal dynamics assuming a linear and balanced system, but did not account for the dynamic mass unbalance which would occur once the body starts rotating [4]. A single axis gimbal which explained the single axis ISP well, but could not extend it to a multiaxis gimbal system is presented in [5]. If one assumes all the nonlinearities present in the system like friction torque or cable restraint torque to be linear or nonexistent, then the derived equations of motion will be an approximation of the actual systems dynamics and not exact [6]. Hence, for such complicated systems one may revert to system identification and parameter estimation techniques. This requires one to perform an experiment or a series of experiments on the actual system and then estimate a model of the system which, due to the advances in computational techniques and computing devices, will give a more accurate model than that obtained mathematical derivation. The motive behind implementing the parameter estimation techniques is to make the ISP system simple by the virtue of mathematical complexity so as to achieve better tuning of the controllers. In addition to that adopting the prediction error method attain that pur-pose better than subspace algorithms and facilitates improved understanding of the gimbal dynamics [7]. System identification was used to find the state space model of

Cite this article as: Majji Nagendra & Sai Ganesh Mopada, "Design and Implementation of Two Axis Gimbal System", International Journal & Magazine of Engineering, Technology, Management and Research, Volume 6 Issue 9, 2019, Page 105-109.

ISSN No: 2348-4845
International Journal & Magazine of Engineering, Technology, Management and Research
A Peer Reviewed Open Access International Journal

the gimbal dynamics, but a balanced gimbal system assumed thereby reducing the complexity of it [8]. Here, an unbalanced gimbal system is modeled and simulated. Then, its parameters are estimated using the prediction error estimation method.

2. Gimbal Dynamic:

The two-axis gimbal is considered as shown in Fig. 1. It is placed on the main body via shock absorbers, and the outer gimbal is the azimuth gimbal and the inner gimbal is the elevation gimbal [1]. The sensor is placed on the inner gimbal, and its velocities in y and z direction are measured with the help of a rate gyro placed on the elevation gimbal. Three sets of coordinate frames are attached to each of the body, azimuth and elevation gimbals, (i, j, k) to the body, (n, e, k) to the outer gimbal, and (r, e, d) to the inner gimbal with A representing the inner gimbal, by representing the outer gimbal and P represents the main vehicle. The coordinate transformation matrices from P to B and B to A are as shown.

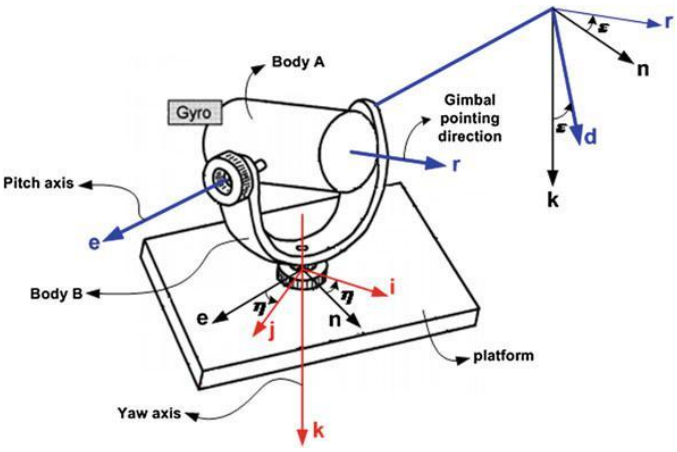

Fig.1: Two-axis inertial stabilization system—axis representation

$$ {}^{B}_{P}C = \begin{bmatrix} \cos\eta & \sin\eta & 0 \\ -\sin\eta & \cos\eta & 0 \\ 0 & 0 & 1 \end{bmatrix} \quad {}^{A}_{B}C = \begin{bmatrix} \cos\varepsilon & 0 & -\sin\varepsilon \\ 0 & 1 & 0 \\ \sin\varepsilon & 0 & \cos\varepsilon \end{bmatrix} \tag{1} $$

Angular velocities are assigned to each frame with respect to coordinate their respective planes. The equations relating the angular velocities of different frames are as follows:

$$ \begin{cases} \omega_{Bn} = \omega_{Pi}\cos\eta + \omega_{pj}\sin\eta \\ \omega_{Be} = -\omega_{Pi}\sin\eta + \omega_{pj}\cos\eta \\ \omega_{Bk} = \omega_{Pk} + \dot{\eta} \end{cases} \tag{2} $$

$$ \begin{cases} \omega_{Ae} = \omega_{Be} + \dot{\varepsilon} \\ \omega_{Ad} = \omega_{Bn}\sin\varepsilon + \omega_{Bk}\cos\varepsilon \\ \omega_{Ar} = \omega_{Bn}\cos\varepsilon - \omega_{Bk}\sin\varepsilon \end{cases} \tag{3} $$

With Eq. (2) representing the transformation between main body and outer gimbal, and Eq. (3) is the relation between outer and inner gimbals angular velocities. The angles η and e are the angles between the outer gimbal and the main body and the inner and outer gimbals, respectively, with e and g representing the rate of change of the angles.

The azimuth and elevation channel relationships are derived using the torque equation from Newton's law

$$ T = J \cdot \alpha \tag{4} $$

This is the case when the plane in which the object is rotated on a stationary frame. When both are rotating, the equation becomes

$$ \bar{T} = \frac{\mathrm{d}}{\mathrm{d}t}\bar{H} + \bar{\omega} \times \bar{H}; \quad \bar{H} = J \cdot \bar{\omega} \tag{5} $$

The angular velocities of the main body, inner, and outer gimbal are given in the following notations based on Fig. 1

$$ {}^{P}\bar{\omega}_{P/I} = \begin{bmatrix} \omega_{Pi} \\ \omega_{Pj} \\ \omega_{Pk} \end{bmatrix}, \quad {}^{B}\bar{\omega}_{B/I} = \begin{bmatrix} \omega_{Bn} \\ \omega_{Be} \\ \omega_{Bk} \end{bmatrix}, \quad {}^{A}\bar{\omega}_{A/I} = \begin{bmatrix} \omega_{Ar} \\ \omega_{Ae} \\ \omega_{Ad} \end{bmatrix} \tag{6} $$

The inertia matrices of the inner and outer gimbal are given under the following notation:

$$ {}^{A}J_{\text{inner}} = \begin{bmatrix} A_r & A_{re} & A_{rd} \\ A_{re} & A_e & A_{de} \\ A_{rd} & A_{de} & A_d \end{bmatrix} \quad {}^{A}J_{\text{outer}} = \begin{bmatrix} B_n & B_{ne} & B_{nk} \\ B_{ne} & B_e & B_{ke} \\ B_{nk} & B_{ke} & B_k \end{bmatrix} \tag{7} $$

The inertia matrix is not diagonal since mass unbalance is taken into consideration. The equation for the angular momentum of the elevation gimbal is as given below represents the moment of inertia of the elevation gimbal:

$$ {}^{A}\bar{H}_{\text{inner}} = {}^{A}J_{\text{inner}}\bar{\omega}_{A/I} = \begin{bmatrix} A_r\omega_{Ar} + A_{re}\omega_{Ae} + A_{rd}\omega_{Ad} \\ A_{re}\omega_{Ar} + A_e\omega_{Ae} + A_{de}\omega_{Ad} \\ A_{rd}\omega_{Ar} + A_{de}\omega_{Ae} + A_{Ad}\omega_{Ad} \end{bmatrix} = \begin{bmatrix} H_r \\ H_e \\ H_d \end{bmatrix} \tag{8} $$

From which the torque acting on the elevation channel of the gimbal is found to be by Eq. (8) in (5).

ISSN No: 2348-4845
International Journal & Magazine of Engineering, Technology, Management and Research
A Peer Reviewed Open Access International Journal

$$A_e\dot{\omega}_{Ae} = T_{EL} + T_{D-EL} \tag{9}$$

$$T_{D-EL} = (A_d - A_r)\omega_{Ar}\omega_{Ad} - A_{re}(\dot{\omega}_{Ar} + \omega_{Ae}\omega_{Ad}) + A_{rd}(\omega_{Ar}^2 - \omega_{Ad}^2) - A_{de}(\dot{\omega}_{Ad} - \omega_{Ae}\omega_{Ar}) \tag{10}$$

$T_{D\text{-}EL}$ is the disturbance torque due to the gimbals inertia.

The load acting on the azimuth gimbal is a combination of both the payload and the elevation gimbal. The torque acting on it is as follows:

$$T = \frac{\mathrm{d}}{\mathrm{d}t}H|_B + \omega_{B/I} \times H \tag{11}$$

$$H = \begin{bmatrix} H_i \\ H_j \\ H_k \end{bmatrix} = {}^{B}J_{\text{outer}}\omega_{B/I} + {}^{A}_{B}C^{TA}J_{\text{inner}}\omega_{A/I} \tag{12}$$

$$H_k = B_{nk}\omega_{Bn} + B_{ke}\omega_{Be} + B_k\omega_{Bk} - (A_r\omega_{Ar} + A_{re}\omega_{Ae} + A_{rd}\omega_{Ad})\sin\varepsilon + (A_{rd}\omega_{Ar} + A_{de}\omega_{Ae} + A_d\omega_{Ad})\cos\varepsilon \tag{13}$$

$$(\omega_{B/I} \times H)_k = \omega_{Bn}(B_{ne}\omega_{Bn} + B_e\omega_{Be} + B_{ke}\omega_{Bk} + A_{re}\omega_{Ar} + A_e\omega_{Ae} + A_{de}\omega_{Ad}) - \omega_{Be}(B_n\omega_{Bn} + B_{ne}\omega_{Be} + B_{nk}\omega_{Bk}) - \omega_{Be}(A_r\omega_{Ar} + A_{re}\omega_{Ae} + A_{rd}\omega_{Ad})\cos\varepsilon - \omega_{Be}(A_d\omega_{Ar} + A_{de}\omega_{Ae} + A_d\omega_{Ad})\sin\varepsilon \tag{14}$$

$$J_{eq}\dot{\omega}_{Bk} = T_{Az} + T_{d1} + T_{d2} + T_{d3} \tag{15}$$

where J_{eq}, T_{d1}, T_{d2}, T_{d3}, and T_{d4} are simplified as

$$J_{eq} = B_k + A_r\sin^2\varepsilon + A_d\cos^2\varepsilon - A_{rd}\sin(2\varepsilon) \tag{16}$$

$$T_{d1} = [B_n + A_r\cos^2\varepsilon + A_d\sin^2\varepsilon + A_{rd}\sin(2\varepsilon) - (B_e + A_e)]\omega_{Bn}\omega_{Be} \tag{17}$$

$$T_{d2} = -[B_{nk} + (A_d - A_r)\sin\varepsilon\cos\varepsilon + A_{rd}\cos(2\varepsilon)] \times (\dot{\omega}_{Bn} - \omega_{Be}\omega_{Bk}) - (B_{ke} + A_{de}\cos\varepsilon - A_{re}\sin\varepsilon) \times (\dot{\omega}_{Be} + \omega_{Bn}\omega_{Bk}) - (B_{ne} + A_{re}\cos\varepsilon + A_{de}\sin\varepsilon) \times (\omega_{Bn}^2 - \omega_{Be}^2) \tag{18}$$

$$T_{d3} = \ddot{\varepsilon}(A_{re}\sin\varepsilon - A_{de}\cos\varepsilon) + \dot{\varepsilon}[(A_r - A_d)(\omega_{Be}\cos(2\varepsilon) - \omega_{Bk}\sin(2\varepsilon))] + \dot{\varepsilon}[2A_{re}(\omega_{Bn}\sin(2\varepsilon) + \omega_{Bk}\cos(2\varepsilon))] + \dot{\varepsilon}[(A_{de}\sin\varepsilon + A_{re}\cos\varepsilon)(\omega_{Ae} + \omega_{Be}) - A_e\omega_{Bn}]. \tag{19}$$

3. Kinetic Coupling

In the above equations, the terms of the type A_{re}, A_{rd}, A_{de} denote the inertia terms of the respective gimbals with respect to two axes and are called as products of inertia. Such terms are zero for symmetrical bodies. In addition to the asymmetrical nature of the ISP, angular coupling between the two channels is also present, meaning that the angular motion with respect to one axis disrupts the position of the LOS with respect to another axis. These two situations were considered while deriving the torque equations. The simulation diagram is shown in Fig. 2.

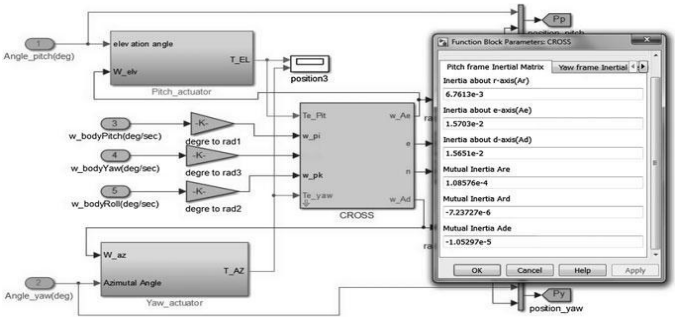

Fig. 2 Simulation diagram of the system with body rates

5. Simulation and Results

The two case studies are estimated with different inputs using system identification toolbox and obtained estimated model and are shown below. Both the original and estimated models are tested with the same input, i.e., unit step and corresponding output signals are observed in each case for elevation, yaw channels and their position, stabilization loops.

Case (i): The estimated state space model with A, B, C, and D is given by

The results corresponding to case (i) are given in Figs. 3, 4, 5, and 6. In which, subplot shows the original system response and (b) subplot shows estimated model response characteristics. From the time and frequency domain characteris-tics, it shows that the estimate system replicates the original system to provide a simplified model to tune the PID controllers.

Case (ii): The estimated state space model with A, B, C, and D is given by

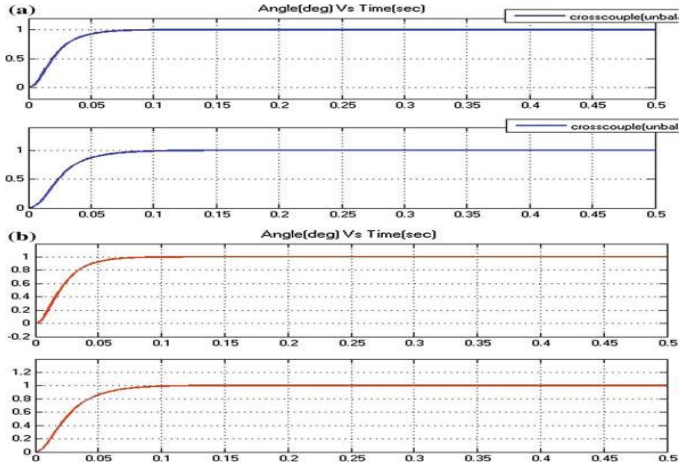

Fig. 3 Step position responses of elevation and yaw channel a cross-coupled, b estimated

ISSN No: 2348-4845
International Journal & Magazine of Engineering, Technology, Management and Research
A Peer Reviewed Open Access International Journal

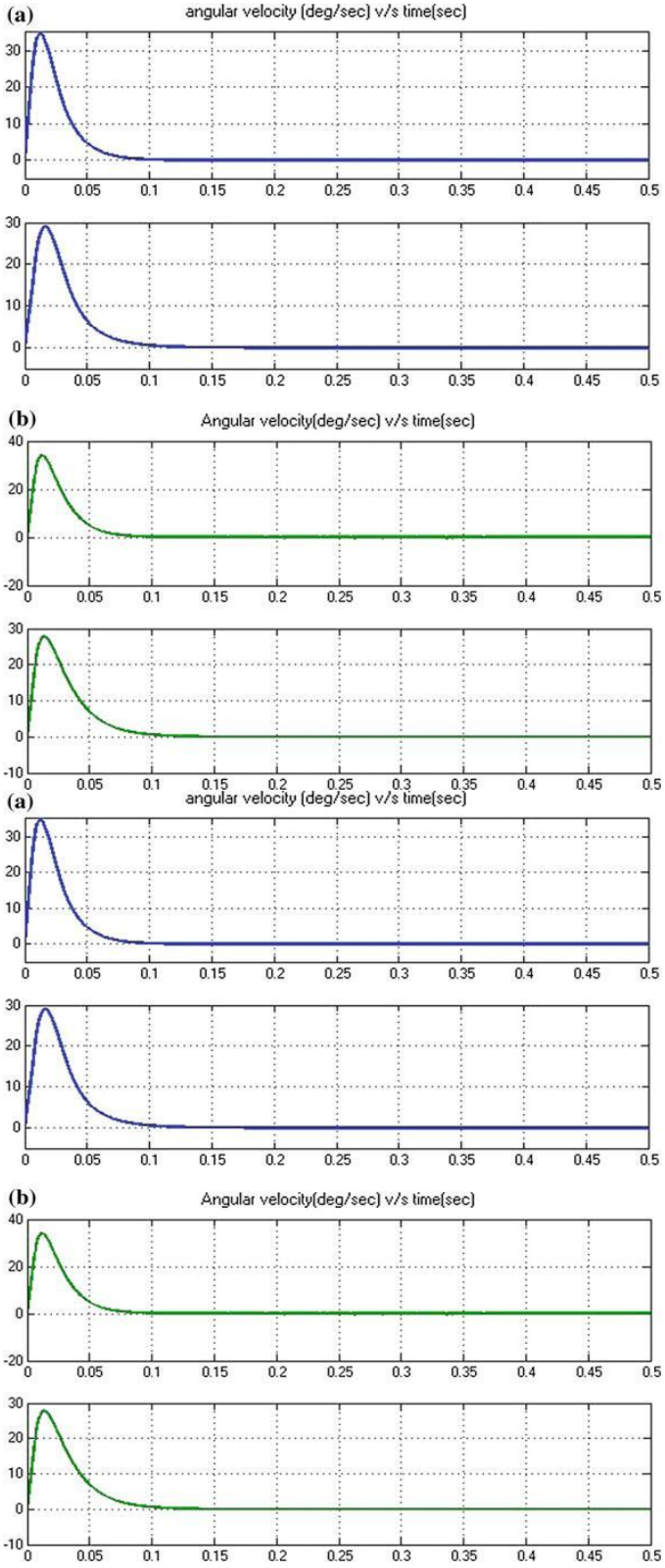

Fig. 4 Stabilization loop responses of elevation and yaw channel a cross-coupled, b estimated

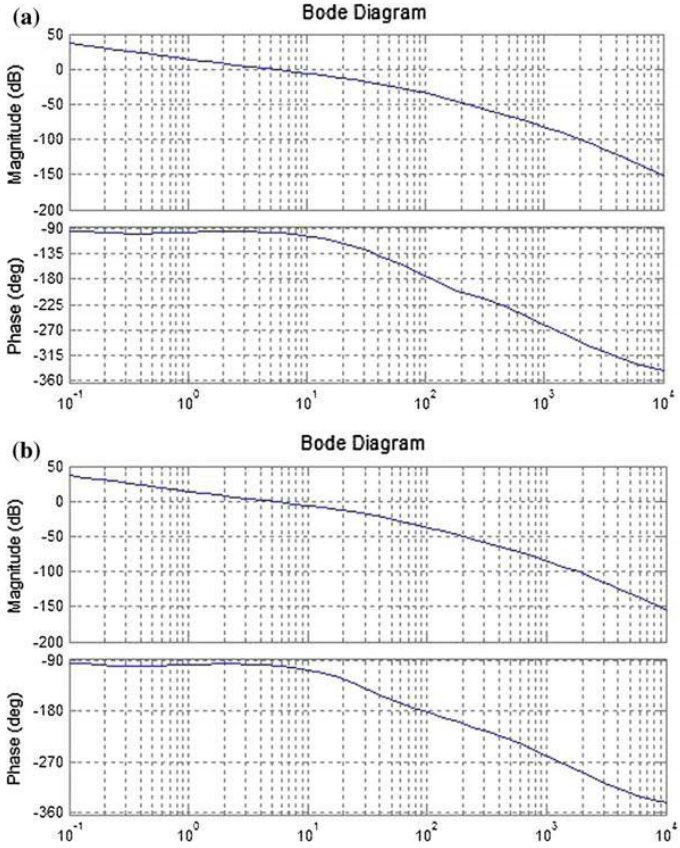

Fig. 5 Frequency responses of elevation position loop a cross-coupled, b estimated

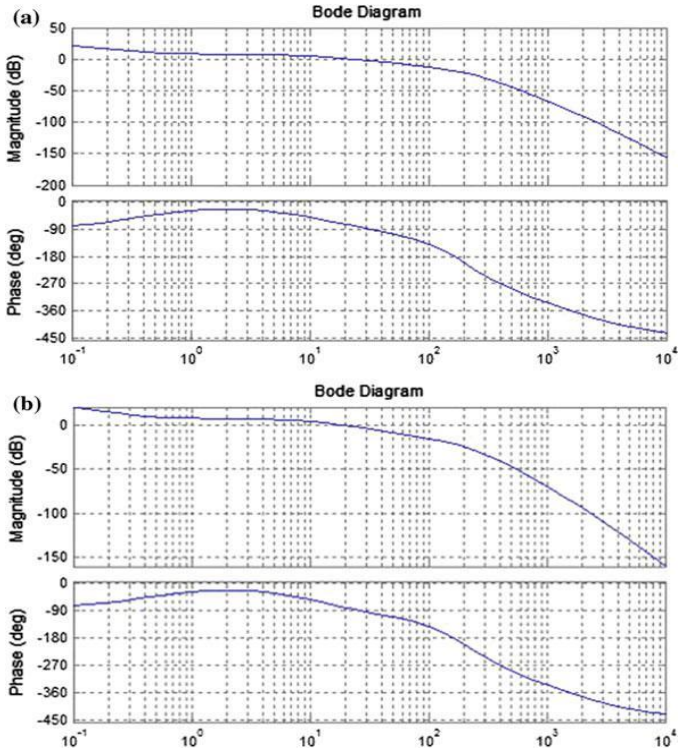

ISSN No: 2348-4845
International Journal & Magazine of Engineering, Technology, Management and Research
A Peer Reviewed Open Access International Journal

References:

[1] Masten M.K. (2008) Inertially stabilized platform for optical imaging systems. IEEE Control Systems Magazine, Vol. 28, pp. 47-64.

[2] Final report (1976) Analytic study of inside-out / coincident gimbal dynamics. The Bendix Corporation, Guidance System Division.

[3] Stokum L.A. and Carroll G.R. (1984) Precision stabilized platform for ship-borne electro-optical systems. SPIE, Vol. 493, pp. 414-425.

[4] Rue A.K. (1974) Precision stabilization systems. IEEE Trans. Aerospace and Electronic Systems, Vol. AES-10, No. 1, pp. 34-42.

[5] Ekstrand B. (2001) Equation of motion for a two axes gimbal system. IEEE Trans. On Aerospace and Electronic Systems, Vol. 37, No. 3, pp. 1083-1091.

[6] Daniel R. (2008) Mass properties factors in achieving stable imagery from a gimbal mounted camera. Published in SPIE Airborne Intelligence, Surveillance, Reconnaissance (ISR) Systems and Applications V, Vol. 6946, doi:10.1117/12.778245.

[7] Yu S. and Zhao Y. (2010) A New measurement method for unbalanced moments in a two axes gimbaled seeker. Chinese Journal of Aeronautics, Vol. 23, No. 1, pp. 117-122.

[8] Özgür H., Aydan E. and İsmet E. (2011) Proxy-based sliding mode stabilization of a two axes gimbaled platform. Proceedings of the World Congress on Engineering and Computer Science, San Francisco, (WCECS), 19-21 October. Vol. I.

[9] Ravindra S. (2008) Modeling and simulation of the dynamics of a large size stabilized gimbal platform assembly. Asian International Journal of Science and Technology in Production and Manufacturing, Vol. 1, No. 2, pp. 111-119.

[10] Khodadadi H. (2011) Robust control and modeling a 2-DOF Inertial Stabilized Platform. International Conference on Electrical, Control and Computer Engineering, Pahang, Malaysia, June 21-22, pp. 223-228. 12 Int. j. adv. robot. syst., 2013, Vol. 10, 357:2013 www.intechopen.com

[11] Hilkert J.M. (2008) Inertially stabilized platform technology. IEEE Control Systems Magazine, Vol. 28, pp. 26-46.

[12] Tang K.Z., Huang S.N., Tan K.K. and Lee T.H. (2004) Combined PID and adaptive nonlinear control for servo mechanical systems. Mechatronics, Vol. 14, pp. 701-714.

[13] Malhorta R., Singh N. and Singh Y. (2010) Design of embedded hybrid fuzzy-GA control strategy for speed control of DC motor: a servo control case study. International Journal of Computer Applications, Vol. 6, No. 5, pp. 37-46.

[14] Ljung, L.: System identification: theory for the user. Prentice-Hall, Englewood Cliffs, NJ (1987).

[15] Ha, J. et al.: A study on the control method of a ship borne launcher using a system identification method. 2015 19th International Conference on System Theory, Control and Computing (ICSTCC). (2015)..